SEARCHING FOR LUNAR HORIZON GLOW USING LROC IMAGES P. Mahanti[1], M.S. Robinson[1], S.D. Thompson[1], D.C. Humm[2], [1]Lunar Reconnaissance Orbiter Camera, School of Earth and Space Exploration, Arizona State University, Tempe,AZ,USA; pmahanti@asu.edu; [2]Space Instrument Calibration Consulting, Annapolis, MD, USA.

Introduction: Observations made from the Clementine Star Tracker Camera images and reported by Zook et al [1], Surveyor 5, 6, 7 and reported by Rennilson et al [2] and sketches by Eugene A. Cernan (Apollo 17 astronaut) were interpreted to indicate the presence of a 'lunar horizon glow' (LHG) before and after local sunrise and sunsets, respectively. The effect is different from Earth-shine and illumination due to Sun's corona and associated Coronal-Zodiacal light (CZL)(Fig. 1). While a similar effect, primarily due to dust is seen for Earth sunsets, such an effect is confounding for the Moon. Accordingly, various theories for its origin and associated simulations have been presented historically [1, 2, 3].

On 20 July 2011, the Lunar Reconnaissance Orbiter Camera (LROC) [4] aboard the LRO spacecraft performed its first series of experiments in an attempt to detect the weak signal of putative LHG. The experiments were scheduled jointly with the Lyman-alpha Mapping Project (LAMP), another instrument onboard the LRO, and more sensitive to changes in photon flux. Observations by the LRO Narrow Angle Camera (NAC) and Wide Angle Camera (WAC) were acquired at very high exposure times (more than 50 times higher than normal for both cameras). Description of the experimental imaging geometry, the image analysis procedures and results is presented in this work.

Experimental imaging geometry: To observe the LHG with LROC and LAMP, the spacecraft was reoriented from nominal nadir position with a 78° roll about its velocity vector (x-axis) and this was maintained for 240 seconds. With LRO rolled 78° from nadir, and at 60 km altitude at time of experiment, the combined NAC crosstrack field of view (FOV) were aligned perpendicular to and ≈1.0 km above the lunar limb (Fig. 2).

The illumination conditions during the experiment were with the Sun having a subsolar longitude of 79°E, the terminator at 169°E longitude, and LRO orbiting along the 192°E longitude. LRO was shadowed by the Moon from the Sun, and was looking back into the region of space across the Sun's rays to observe material that exhibits forward-scattering reflectance.

Image data analysis: The NAC has a single line CCD, multiple lines acquired temporally form an image. Hence the line direction represents a spatial change along the lunar surface. For the WAC, a single frame is acquired at a time, and many frames form an image. Each of these frames have 2 UV bands and

Figure 1: Images from Clementine Star Tracker camera. The first and third images shows predominant Earth-shine and solar corona,respectively. The second image was interpreted to indicate a lunar limb associated component.

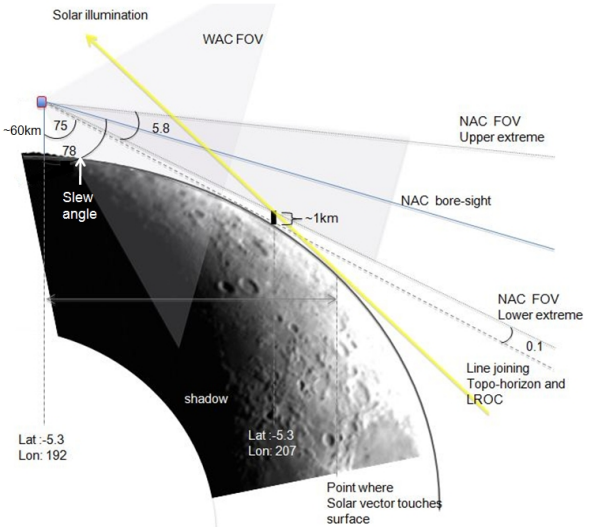

Figure 2: Imaging geometry for the LROC. Lower end of the NAC FOV is just above and sample direction increases away from lunar surface.

5 visible bands, separated spatially on the CCD array. During pre-processing, raw NAC data (experimental image M165764925 and corresponding dark image M165765151) was first corrected with masked pixel subtraction and then the dark image was subtracted from the experimental image. Similarly, the 3 experimental images for the WAC were also calibrated and dark subtracted, and these contribute 78 (20+24+34) frames in time direction.

Analysis of the limb observations was performed by first segmenting the image into regions. Details of this are shown in Fig. 3. Median DN values from these regions are then collected into a time series based on the line position (NAC) and frame position (WAC). Elevation from the lunar surface increases with sample direc-

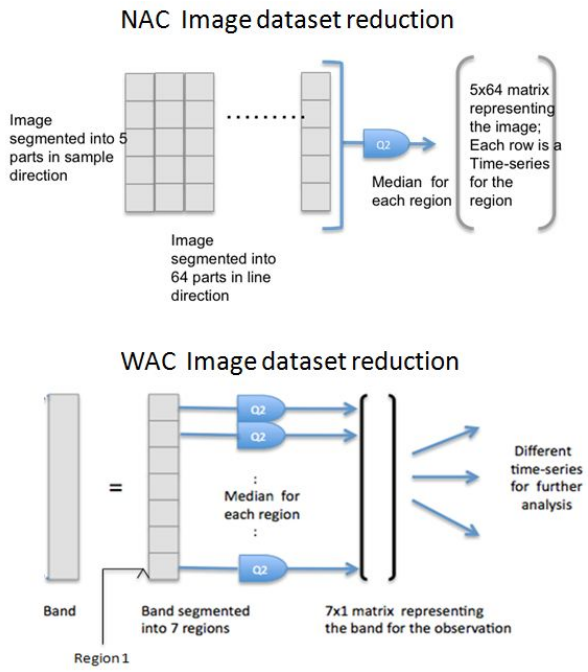

Figure 3: LROC image data analysis. A NAC image is subdivided into 64 regions in line and 5 in sample direction. Median DN value is obtained for every region resulting in a 5x64 matrix. Each WAC image frame (for a specific band) is subdivided into 7 regions in the sample direction and the first region in each frame represents a time series point in the results.

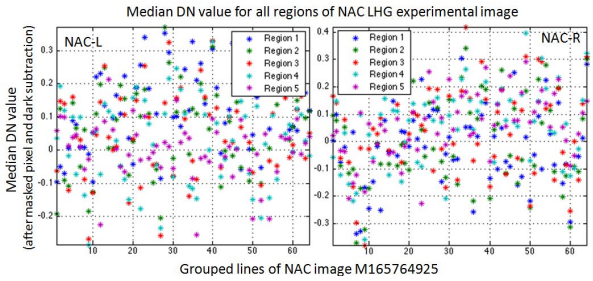

Figure 4: An example result from the NAC image.

tion, and accordingly region 1 is closest to the surface for both cameras.

Results from image data analysis: The NAC data analysis (Fig. 4) shows the calibrated residual DN values for both NAC's at 35ms exposure (60 times higher than normal). The signal is found to vary between $\pm$ 0.4 DN's with a median value of 0.059 for NACL and 0.028 for NACR. No variations were observed between different regions.

For the WAC (Fig. 5), the dark calibrated DN values for the experimental images are less than $\pm$ 0.8 DN's for all the 3 images. Region 1 (closest to the lunar surface for the roll slew) is shown for all the 78 frames and for all the visible bands. DN levels for UV bands were even

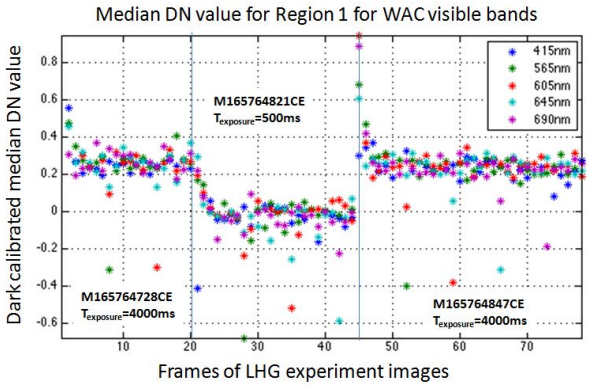

Figure 5: Result from the WAC images, by arranging the frames as time-series.

lower and not shown here. The difference in DN level between M165764821CE and the other two images is consistent with dark level in the image having a residual dependence on exposure time, and does not indicate the presence of LHG.

Conclusion: LROC NAC and WAC images were taken with very high exposure times, looking at a region of space above the limb and outside the Moon's shadow. No lunar horizon glow was detected. For the NAC, the mean counts were 0.03 DN, indistinguishable from dark. For 35 ms exposure time, LHG with spectral radiance of 0.01 W/m2/sr/um would have been detected by the NAC, so for the given observing geometry the LHG, if it exists, must be dimmer than 0.01 W/m2/sr/um. This is a very conservative value and takes into account the NAC nonlinearity, which causes it to be relatively insensitive at low signal levels.

For the WAC, the residual signals were only 0.2 DN with 4 s exposure time and 0.0 DN with 0.5 s exposure time. The difference is likely due to changes in the dark images for different exposure times.

It may be noted that optimal acquisition of horizon glow data depends on many factors including spacecraft and sun position, exposure times, the height of the FOV above the lunar surface, and the absence of scattered light. The analysis methods and tools developed in this study will be useful for future attempts to observe lunar horizon glow.

References: [1] H. Zook, et al. (1991) *Geophysical Research Letters* 18(11):2117. [2] J. Rennilson, et al. (1974) *Earth, Moon, and Planets* 10(2):121. [3] T. Stubbs, et al. (2008) in *Lunar and Planetary Institute Science Conference Abstracts* vol. 39 2378. [4] M. Robinson, et al. (2010) *Space science reviews* 150(1):81.